ELSEVIER

www.elsevier.nl/locate/carres

Carbohydrate Research 321 (1999) 96–104

CARBOHYDRATE RESEARCH

Conformations and lipophilicity profiles of some cyclic β-(1→3)- and β-(1→6)-linked oligogalactofuranosides☆

Holger Gohlke, Stefan Immel, Frieder W. Lichtenthaler *

Institut für Organische Chemie, Technische Universität Darmstadt, Petersenstraße 22, D-64287 Darmstadt, Germany

Received 26 April 1999; accepted 2 July 1999

Abstract

The conformational features of cyclooligosaccharides composed of β-(1→3)- and β-(1→6)-linked galactofuranose units, i.e., *cyclo*[D-Gal*f*β-(1→3)]$_n$ with $n=4$ (**1**) and 5 (**2**), and *cyclo*[D-Gal*f* β-(1→6)]$_n$ with $n=3$ (**3**) and 4 (**4**), were investigated by means of Monte Carlo simulations. The flexibility of the macrocyclic backbone strongly favors bent and asymmetrical conformations over round geometries. Generation of the molecular surfaces of the global minimum-energy structures reveals disk-type shapes for **1**–**4** without through-going central cavities, yet distinct indentations close to the O-2/O-3 groups, respectively. The molecular lipophilicity patterns prove these surface dents to be hydrophobic for the β-(1→6)-linked cyclogalactans **3** and **4**, whereas their β-(1→3)-linked counterparts display an inverse situation with a hydrophobic outer core structure.

Keywords: Oligogalactosides, cyclic; Cyclodextrin analogs; Cyclogalactofuranosides

1. Introduction

The starch-derived cyclodextrins with six, seven, and eight α-(1→4)-linked glucopyranose units have enjoyed a preeminent position in supramolecular chemistry as their capability to form inclusion complexes and, hence, to function as enzyme models has contributed substantially to our understanding of molecular recognition processes in general, and enzyme reactions in particular [2]. Their macrocycles are characterized by a remarkable structural rigidity, such that they are capable of mimicking the classic lock-and-key concept of enzyme specificity [3] rather than the more realistic induced-fit mode [4], which entails guest-induced conformational changes toward a transition state geometry.

Several options have been realized — by synthetic means invariably — to introduce flexibility into the common, overly rigid cyclodextrins. Thus, the α-(1→4) linkup of the glucopyranose residues has been changed to α-(1→6) [5] and β-(1→6) [6] connections, thereby 'elongating' the intersaccharidic link from a singular oxygen to an O–CH_2 joint; unfortunately, the respective cyclooligosaccharides have only been characterized as their benzyl ethers [5] or peracetates [6] and, except for a dimer [7], hardly any information is available on the conformation of their macrocycles [5b]. Configurational inversion of the glucose-2-OH in the cyclodextrins, resulting (formally) in the cyclomannins [8], had little

☆ Molecular modeling of saccharides, Part 22. For Part 21, see Ref. [1]. — Presented in part at the 9th International Symposium on Cyclodextrins, Santiago de Compostela, Spain, May 1998, Abstract 2-P-4.

* Corresponding author. Tel.: +49-6151-162-376; fax: +49-6151-166-674.

E-mail address: fwlicht@sugar.oc.chemie.tu-darmstadt.de (F.W. Lichtenthaler)

0008-6215/99/$ - see front matter
PII: S0008-6215(99)00174-3

effect on the flexibility of the macrocycles, as the $^4C_1$ geometry of the pyranoid rings is rigid enough to be retained [9] — a state that also holds for the cyclorhamnins [10,11] and for cyclooligosaccharides with alternating L-rhamnose and D-mannose units [12].

The first non-glucose cyclooligosaccharides with substantial macrocyclic flexibility proved to be those containing altrose residues, i.e., cyclodextrins in which the configuration at C-2 and C-3 has been inverted: mono-*altro*-β-cyclodextrin undergoes conformational changes in its altrose moiety upon inclusion of adamantane-carboxylate [13], and the cycloaltrins composed of six [14], seven [15], and eight [16] α-(1→4)-linked D-altropyranose units are thoroughly flexible, adopting a variety of macrocyclic conformations in solution [1].

As furanoid rings display a higher pseudorotational mobility than their pyranoid counterparts, cyclooligosaccharides composed of furanoid sugar units are apt to be more flexible in their macrocycle. This expectation, however, has not materialized in the inulin-derived [17] cyclofructins; their six, seven, or eight β-(1→2)-linked fructofuranose units are spiro-anellated onto a crown-ether backbone thereby conferring rigidity on their macrocycles [18]. By contrast, the cyclogalactans composed of β-(1→3)-, β-(1→5)-, and β-(1→6)-linked galactofuranose units (Scheme 1) — in fact the first non-glucose cyclooligosaccharides prepared synthetically [19] — are likely to provide larger macrocyclic flexibility, not only due to the higher pseudorotational mobility of the furanoid rings, but as a consequence of, in the β-(1→6)-linked species in particular, the larger number of atoms bridging the furanose residues and the steric strain imposed by the respective macrocyclic assemblies.

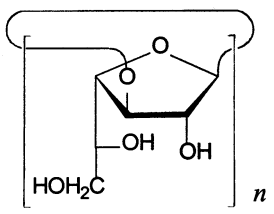

cyclo[D-Gal*f* β(1→3)]$_n$
n = 3,4

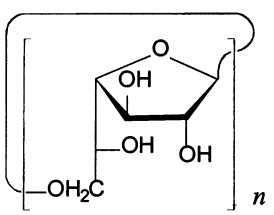

cyclo[D-Gal*f* β(1→6)]$_n$
n = 2 - 9

Scheme 1.

Due to the rather modest yields in their preparation by cycloglycosylation of tritylated 1,2-*O*-(1-cyano)ethylidene derivatives of D-galactofuranose [19], neither the molecular geometries of these cyclogalactans nor their capabilities to form inclusion complexes were investigated. In view of their potential to function as flexible hosts in molecular recognition processes, we have initiated a molecular modeling study, for which we selected, as examples, the tetra- and pentamer of the β-(1→3)-cyclogalactofuranosides **1** and **2**, and, due to their higher flexibility, the trimer (**3**) and tetramer (**4**) of the β-(1→6)-type analogs (Scheme 2).

2. Results and discussion

Conformational analysis of β-D-galactofuranose.—Since comparatively few furanoid ring systems of pentoses and hexoses have been analyzed in detail — D-ribose, 2-deoxy-D-ribose [20], D-arabinose [21], D-fructofuranose [22], and D-psicose [23] are notable examples — a pre-condition for elaborating the molecular geometries of furanoid cyclogalactans was a detailed conformational assessment of their building unit, i.e., β-D-galactofuranose itself. The adiabatic energy potential surface of the ring conformations of β-D-galactofuranose, determined using the PIMM91 force field [24], reveals a single, broad energy minimum in the western part of the pseudorotational turntable within the $^4T_3 \rightleftharpoons {}^4E \rightleftharpoons {}^4T_0 \rightleftharpoons E_0$ region for the furanose rings (cf. Fig. 1). This distinct preference for the western part of the Cremer–Pople parameter [25] plot (q/ϕ plane) is obviously due to the opposite tendency of the bulky exocyclic substituent at C-4 and the anomeric OH to occupy pseudoequatorial and pseudoaxial orientations towards the ring, respectively.

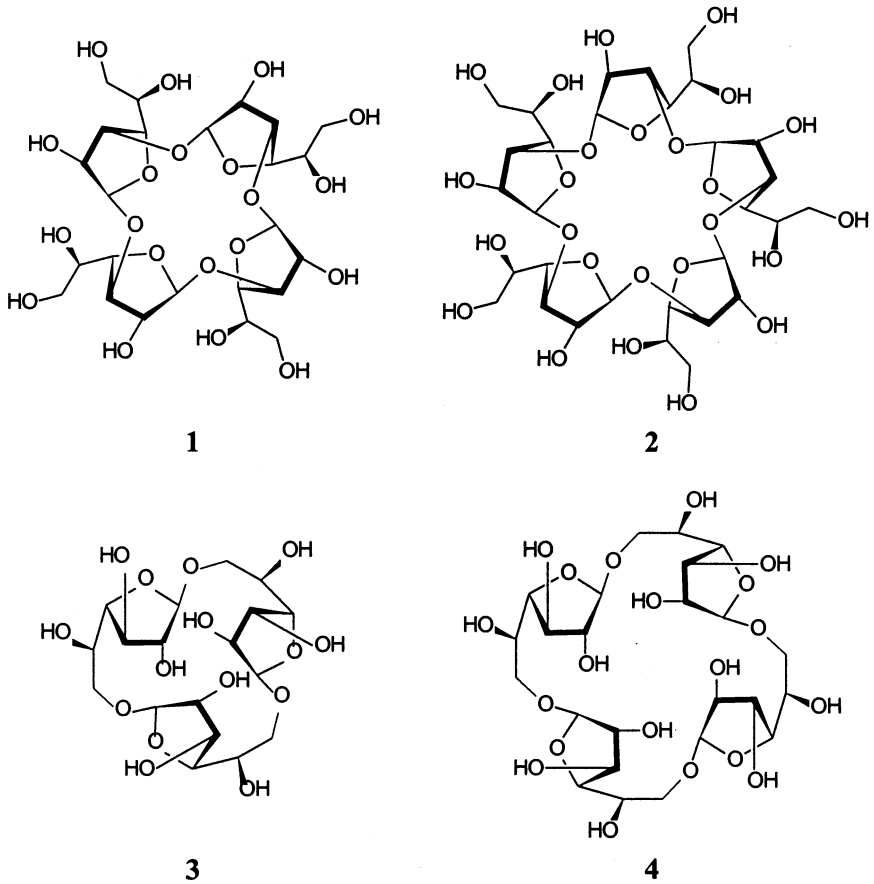

Scheme 2.

The three β-D-galactofuranose structures in the CCDF data file [26], i.e., compounds **5** [27], **6**[1] [28], and **7**[1] [29] (Scheme 3), have ${}^1T_0 \rightleftharpoons {}^1E \rightleftharpoons {}^1T_2$ geometries. Thus, the conformational preference of the furanoid ring in the highly O- and C-substituted galactose derivatives **5**–**7** with different anomeric substituents is only slightly shifted from the ${}^4E$ global minimum for the unsubstituted β-D-galactofuranose (Fig. 1) — a reasonable agreement between in vacuo force-field calculations and crystal structure results.

Further supportive evidence for the relevance of the in vacuo geometries calculated can be derived [30] from the ^{1}H NMR $^3J_{H-H}$ coupling constants of 31 β-D-galactofuranose derivatives[2] described in the literature [27–31], as the majority (22) of their furanoid solution geometries fall into the ${}^4E \rightleftharpoons {}^4T_0 \rightleftharpoons E_0 \rightleftharpoons {}^1T_0$ range, i.e., into the western part of the pseudorotational itinerary within 10 kJ/mol above the force-field-derived global energy minimum depicted in Fig. 1. This congruence of computational and ^{1}H NMR-derived data attests to the relevance of the furanoid geometries obtained by either of the two methods.

Molecular geometries of the cyclooligogalactosides **1**–**4**.—For generation of the macrocyclic geometries of **1**–**4**, a pre-optimized galactofuranose unit was used to construct various symmetrical and asymmetrical starting structures, which were then subjected to conformational analysis using Monte Carlo and Random Walk techniques [32] to search for the global energy minimum of each compound. An adapted corner-flipping procedure [33] was used to effectively vary the ring geometries of the furanose units as well as of the macrocyclic backbone without breaking bonds

[1] The furanoid ring conformation for **6** is incorrectly given as ${}^4E$ in Ref. [28]; the ring geometry of **7** was reconstructed from Ref. [29] due to missing 3D-coordinates in the database.

[2] A detailed discussion and conformational evaluation of these β-D-galactofuranose derivatives on the basis of the coupling patterns (mainly in $CDCl_3$, yet some in D_2O, acetone-d_6 and pyridine-d_5) is contained in Ref. 31.

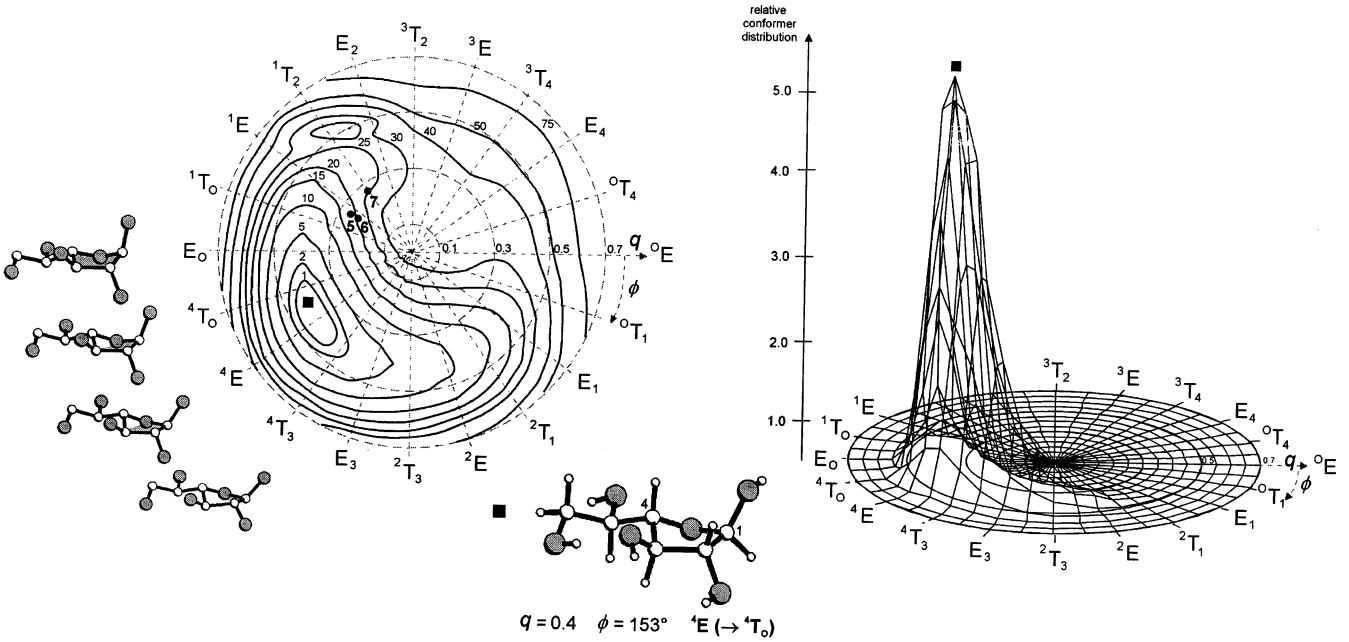

Fig. 1. Left: Adiabatic energy map of β-D-galactofuranose as a function of the Cremer–Pople parameters [25] — i.e., the puckering amplitude q and the phase angle ϕ — calculated by molecular mechanics using the PIMM91 [24] force field. The bold-faced square marks the global energy minimum corresponding to the conformation displayed underneath (^4E form slightly distorted towards the $^4T_0$ geometry), the structures to the left represent the furanose conformations within the $^4T_3 \rightleftharpoons E_0$ range of the pseudorotational turntable. The solid-state conformations of **5**–**7** are indicated by the solid points on the energy potential surface. Right: a 3D plot of the relative Boltzmann distribution of conformers calculated for $T = 300$ K, indicating finite conformer probabilities within the 10 kJ/mol level.

in the different rings. From these extensive procedures, the global minimum-energy structures for the cyclogalactans emerged as ^1E for the preferred furanose geometry of the β-(1→3)-linked species **1** and **2**, versus the $^4T_3$ envelope form for the β-(1→6) analogs **3** and **4**[3]. Although the furanose ring shapes in **1**–**4** appear to be high in energy as they are located approximately +15 kJ/mol above the global minimum of the β-D-galactofuranose energy potential surface (Fig. 1), these structures reflect the different types of substitution of the five-membered rings [free furanose versus β-(1→3)- and β-(1→6)-linkages] (Fig. 2). In toto, the experimental (solid-state structures and NMR) and computational data both point towards preferred furanose geometries in the western part of Fig. 1.

The high flexibility of the furanoid rings, most notably in the β-(1→6)-linked species in **3** and **4** with four torsion angles involved, leads to structures of low symmetry being favored with increasing ring size of the macrocycles. The energy-minimum geometries of **1**–**4** displayed in Fig. 3 show that the small ring homologs **1** and **3** retain symmetry as much as possible (C_4 and C_3, respectively), but **2** and **4** prefer C_1 (asymmetric) and C_2-type structures.

In the case of **3**, and to a lesser extent in **4**, the conformational symmetry is only retained through favorable intramolecular hydrogen bonding interactions of the 3-OH···O-6 and 5-OH···O-4′ type. As in aqueous solutions, these effects are expected to become less important, conceivable conformational equilibria are likely to be shifted towards asymmetric forms.

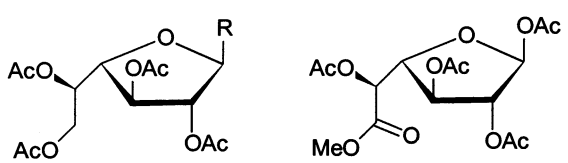

5 R = NO_2
6 R = CN

7

Scheme 3.

[3] The 3D structures can be viewed at http://caramel.oc.chemie.tu-darmstadt.de/immel/3Dstructures.html; MOLCAD graphics are available at http://caramel.oc.chemie.tu-darmstadt.de/immel/molcad/gallery.html.

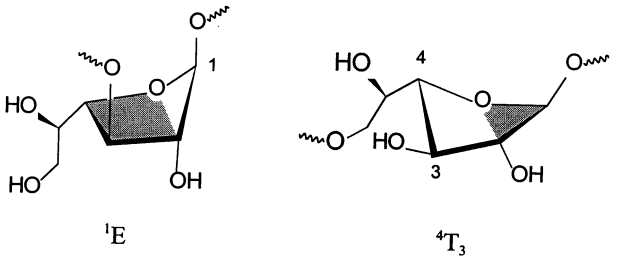

^1E $^4T_3$

Fig. 2. Schematic representation of the furanose geometries calculated for cyclogalactofuranosides **1**–**4**: ^1E conformation for the β-(1→3)-linked cyclooligosaccharides **1** and **2** vs. $^4T_3$ form for the β-(1→6) analogs **3** and **4**.

The molecular contact surfaces computed for **1**–**4** as well as the corresponding surface cross-section cuts (cf. Fig. 3), provide evidence for the disk-type shapes of these macrocycles with small puckering amplitudes (i.e., out-of-plane deviations of ring atoms between the furanose units) of less than 0.5 Å along their backbones. The surface models not only display the effective steric extensions of these molecules and their lack of central cavities to form inclusion complexes, but also allow the mapping of their lipophilicity patterns in color-coded form, as has already proved useful in earlier studies to assess the properties of cyclodextrins [34] and related compounds [11].

Molecular lipophilicity patterns (MLPs).— Besides the steric demands in **1**–**4**, their hydrophobic characteristics are of major interest to evaluate their properties. In Fig. 4, the corresponding MLPs were computed and mapped in color-coded form onto the contact surfaces of Fig. 3. Most remarkably, these graphics reveal a fundamental difference in the distribution of hydrophilic and hydrophobic surface areas for both classes of the β-(1→3)- and β-(1→6)-linked cyclogalactans. In the former case, i.e., **1** and **2** (Fig. 4, top), the surface is significantly indented in the center without elaborating 'through-going' central cavities. Due to their association with the O^1–C^2H–C^3H fragments of the galactofuranose moieties, these surface dents are remarkably hydrophobic, whereas O-4 and the side chain 5-OH and 6-OH groups render the opposite molecular sides much more hydrophilic. Most notably, the outer rim of the disk-shaped molecules carrying the 2-OH hydroxyls is predominantly hydrophilic.

A different situation prevails for the β-(1→6)-cyclogalactosides **3** and **4** (Fig. 4, bottom): the type of intersaccharidic linkage, their increased flexibility, and the altered orientation of the furanoid rings in relation to the macrocycle cause an inverse alignment of hydrophilic and hydrophobic surface regions. As the 5-OH groups are directed towards the central surface dents, they provide a hydrophilic environment that is augmented by the 3-OH groups, whereas on the back the close alignment of the O-4 ring atoms contributes to the slightly less hydrophilic regions. The most hydrophobic surface areas of **3** and **4** are situated on the outer edge of the macrocycles, and are made up by the C^1H, C^3H, and C^5H–C^6H_2 fragments.

In sum, this molecular modeling study of the furanoid cyclogalactans **1**–**4** provides reliable insights into their molecular architecture, such that they not only lack round geometries — the circular shapes depicted in the chemical formulae for **1**–**4** are grossly misleading — but also central cavities with which to form inclusion complexes similar to those given by the cyclodextrins. At most, the formation of loose sandwich-type adducts is conceivable. The larger homologs of the β-(1→6)-cyclogalactosides, however — from the hexamer on, presumably — should be capable of adopting a plethora of macrocyclic conformations in solution, including some with a through-going cavity, from which a guest may select the one most suited for its inclusion. Thus, these galactofurano-cyclooligosaccharides are apt to evolve into attractive flexible models for mimicking the dynamic induced-fit mode of molecular recognition, once they become accessible on a scale to study their supramolecular properties.

3. Experimental

All calculations were carried out using the PIMM91 force-field [24] program with external conformational search algorithms [35], which has been shown [36] to accurately reproduce anomeric and exoanomeric effects. A dielectric constant of $\varepsilon = 1.0$ was used for all calculations without the implicit incorporation

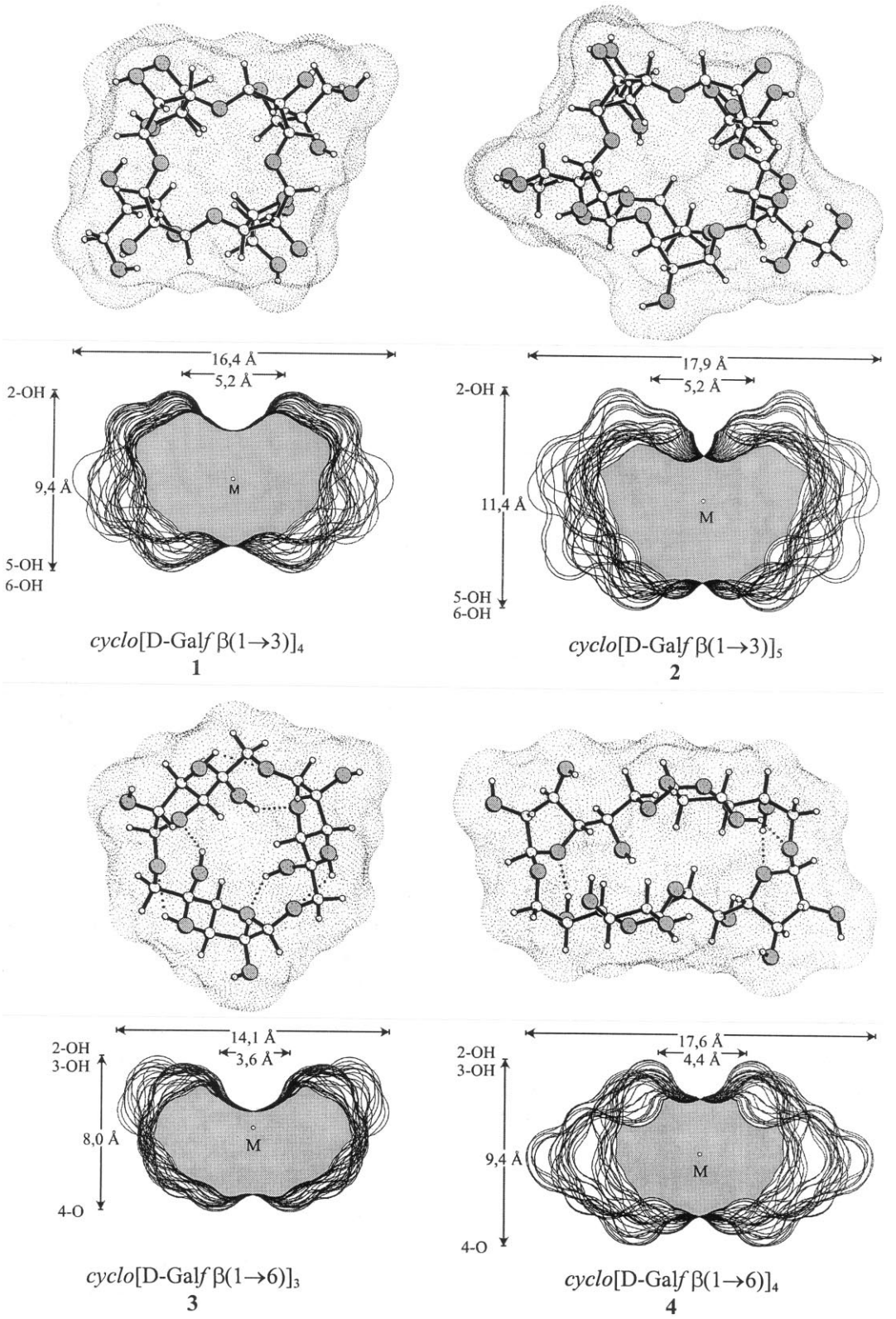

Fig. 3. Global minimum-energy structures of the cyclogalactofuranosides **1**–**4** with their contact surfaces in dotted form; intramolecular hydrogen bonding interactions are indicated by bold dots. All structures are displayed perpendicular to the macrocycles with the O-2/O-3 sides facing the viewer. In addition, surface cross-section plots are shown with approximate molecular dimensions in Å; cross-cuts were obtained from the intersection of molecular surfaces with a rotating plane (360° in steps of 10°) perpendicular to the mean macro-ring planes, and superimposed.

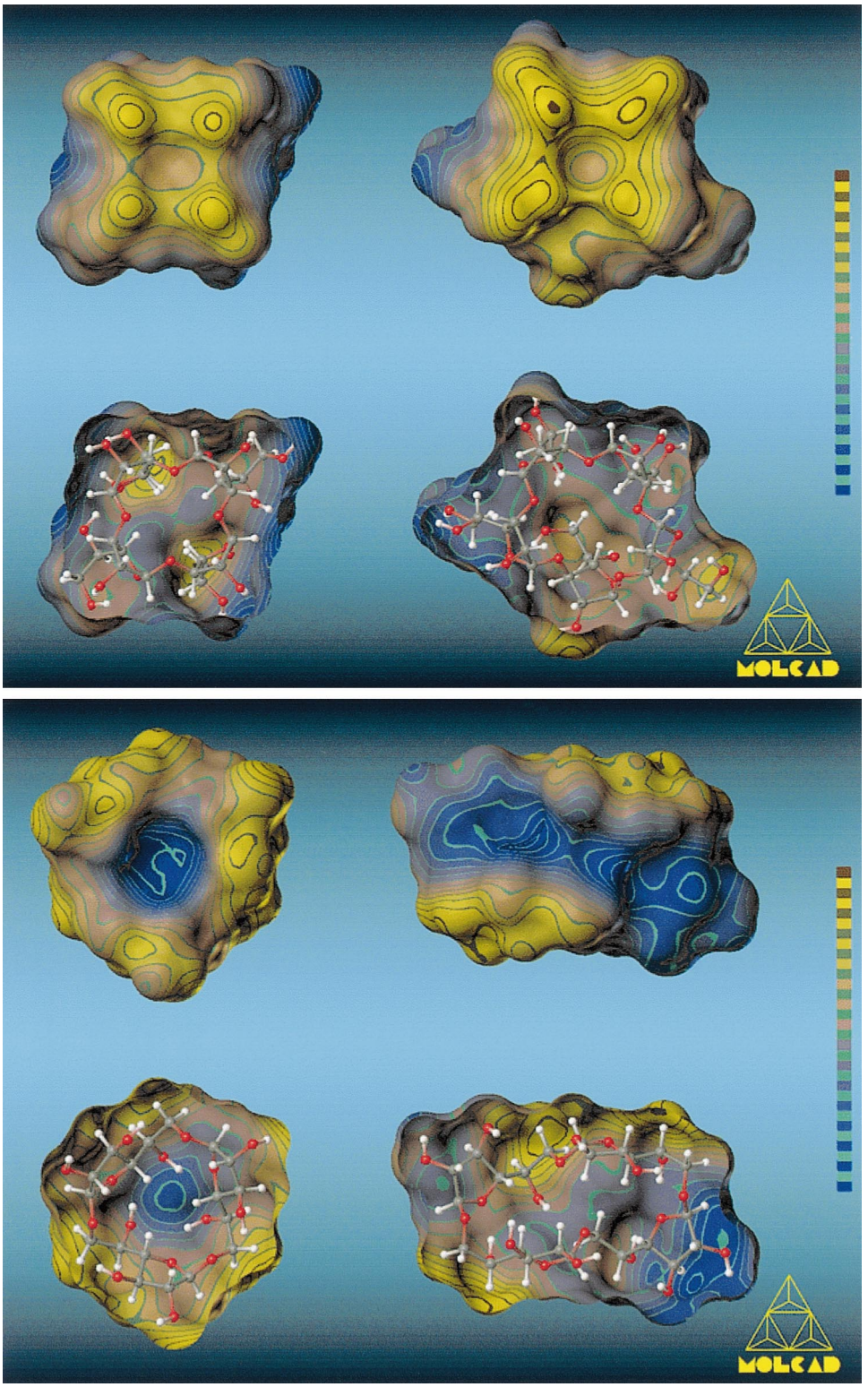

Fig. 4. MOLCAD program-generated molecular lipophilicity patterns (MLPs) projected onto the contact surfaces of the β-(1→3)-(top: **1** and **2**) and β-(1→6)-linked cyclogalactofuranosides (bottom: **3** and **4**). The color code was adapted to the range of relative hydrophobicity calculated for each molecule, ranging from dark-blue for the most hydrophilic areas to full yellow corresponding to the most hydrophobic surface regions. The orientation of all models is such that the O-2/O-3 atoms face the viewer (cf. Fig. 3), whereas the furanoid ring oxygens (O-4) are directed toward the rear; the half-opened models on the bottom each visualize the molecular orientation as well as the surface properties of the rear side.

of solvent models. A pre-optimized galactofuranose unit was assembled to various symmetrical and asymmetrical starting structures of the cyclogalactofuranosides **1**–**4**, which were then subjected to conformational analysis using Monte Carlo and Random Walk simulations [32]. An adapted corner-flapping procedure [33] was used to effectively vary the ring geometries of the furanose units as well as the macrocyclic backbone without breaking bonds in the different rings; all exocyclic torsion angles (–OH and –CHOH–CH_2OH groups) were treated as flexible. Proper sampling of the conformational space was ensured by converging global minimum-energy structures and molecular parameters. For the global minimum-energy structures obtained, the molecular contact surfaces [37], cross-section cuts (Fig. 3) [35], and lipophilicity patterns (MLPs, Fig. 4) [38] were computed; color-coded representations were generated using the MOLCAD [38] modeling program. Color-coded projection of the MLPs onto the corresponding contact surfaces was done by applying texture mapping strategies [39], using a two-color code graded into 32 shades, ranging from dark-blue for the most hydrophilic to yellow for the most hydrophobic areas. Scaling of the MLP profiles was performed in arbitrary units and in relative terms for each molecule separately (from most hydrophilic to most hydrophobic surface regions); no absolute values are displayed. Color graphics were photographed from the computer screen of a Silicon-Graphics workstation.

Acknowledgements

We thank the Fonds der Chemischen Industrie for support of this investigation and Professor Dr J. Brickmann, Institut für Physikalische Chemie, Technische Universität Darmstadt, for providing us with the MOLCAD molecular modeling software package.

References

[1] S. Immel, K. Fujita, F.W. Lichtenthaler, *Chem. Eur. J.*, 5 (1999) in press.

[2] J. Szejtli, T. Osa (Eds.), *The Cyclodextrins*, *Comprehensive Supramolecular Chemistry*, Vol. 3, Pergamon, Oxford, UK, 1996, 626 pp.

[3] (a) E. Fischer, *Ber. Dtsch. Chem. Ges.*, 27 (1894) 2985–2993. (b) F.W. Lichtenthaler, *Angew. Chem.*, 106 (1994) 2456–2467; *Angew. Chem., Int. Ed. Engl.*, 33 (1994) 2364–2374.

[4] D.E. Koshland, Jr., *Angew. Chem.*, 106 (1994) 2368–2372; *Angew. Chem., Int. Ed. Engl.*, 33 (1994) 2375–2378.

[5] (a) S. Houdier, P.J.A. Vottéro, *Carbohydr. Res.*, 248 (1993) 377–384; *Angew. Chem., Int. Ed. Engl.*, 33 (1994) 354–356. (b) S. Houdier, P.J.A. Vottéro, *Carbohydr. Lett.*, 1 (1994) 13–18.

[6] (a) D. Gagnaire, M. Vignon, *Carbohydr. Res.*, 51 (1976) 140–144. (b) D. Bassieux, D. Gagnaire, M. Vignon, *Carbohydr. Res.*, 56 (1977) 19–33. (c) G. Bonas, G. Excoffier, M. Paillet, M. Vignon, *Recl. Trav. Chim. Pays-Bas*, 108 (1989) 259–261.

[7] (a) D. Gagnaire, S. Pérez, V. Tran, *Carbohydr. Res.*, 82 (1980) 185–194. (b) E. Duée, A. Grand, V. Tran, *Acta Crystallogr., Sect. B*, 37 (1981) 850–857.

[8] (a) M. Mori, Y. Ito, T. Ogawa, *Carbohydr. Res.*, 192 (1989) 131–146. (b) M. Mori, Y. Ito, J. Izawa, T. Ogawa, *Tetrahedron Lett.*, 31 (1990) 3191–3194.

[9] F.W. Lichtenthaler, S. Immel, *Tetrahedron: Asymmetry*, 5 (1994) 2045–2060.

[10] (a) M. Nishizawa, H. Imagawa, Y. Kan, H. Yamada, *Tetrahedron Lett.*, 32 (1991) 5551–5554. (b) M. Nishizawa, H. Imagawa, K. Kubo, Y. Kan, H. Yamada, *Synlett*, (1992) 447–448. (c) M. Nishizawa, H. Imagawa, E. Morikuni, S. Hatekayama, H. Yamada, *Chem. Pharm. Bull.*, 42 (1994) 1356–1365.

[11] For a review, see: F.W. Lichtenthaler, S. Immel, *J. Incl. Phenom. Mol. Recognit. Chem.*, 25 (1996) 3–16.

[12] (a) P.R. Ashton, C.L. Brown, S. Menzer, S.A. Nepogodiev, J.F. Stoddart, D.J. Williams, *Chem. Eur. J.*, 2 (1996) 580–591. (b) P.R. Ashton, S.J. Cantrill, G. Gattuso, S. Menzer, S.A. Nepogodiev, A.N. Shipway, J.F. Stoddart, D.J. Williams, *Chem. Eur. J.*, 3 (1997) 1299–1314.

[13] K. Fujita, W.-H. Chen, D.-Q. Yuan, Y. Nogami, T. Koga, T. Fujioka, K. Mihashi, S. Immel, F.W. Lichtenthaler, *Tetrahedron: Asymmetry*, 10 (1999) 1689–1696.

[14] Y. Nogami, K. Nasu, T. Koga, K. Ohta, K. Fujita, S. Immel, H.J. Lindner, G.E. Schmitt, F.W. Lichtenthaler, *Angew. Chem.*, 109 (1997) 1987–1991; *Angew. Chem., Int. Ed. Engl.*, 36 (1997) 1899–1902.

[15] K. Fujita, H. Shimada, K. Ohta, Y. Nogami, K. Nasu, *Angew. Chem.*, 107 (1995) 1783–1784; *Angew. Chem., Int. Ed. Engl.*, 34 (1995) 1621–1622.

[16] Y. Nogami, K. Fujita, K. Ohta, K. Nasu, H. Shimada, C. Shinohara, T. Koga, *J. Incl. Phenom. Mol. Recognit. Chem.*, 25 (1996) 53–56.

[17] (a) M. Kawamura, T. Uchiyama, T. Kuramoto, Y. Tamura, K. Mizutani, *Carbohydr. Res.*, 192 (1989) 83–90. (b) M. Sawada, T. Tanaka, Y. Takai, T. Hanafusa, T. Taniguchi, M. Kawamura, T. Uchiyama, *Carbohydr. Res.*, 217 (1991) 7–17.

[18] (a) S. Immel, F.W. Lichtenthaler, *Liebigs Ann. Chem.*, (1996) 39–44. (b) S. Immel, G.E. Schmitt, F.W. Lichtenthaler, *Carbohydr. Res.*, 313 (1998) 91–105.

[19] L.V. Backinowsky, S.A. Nepogodiev, N.K. Kochetkov, *Carbohydr. Res.*, 185 (1989) C1–C3; *Tetrahedron*, 46 (1990) 139–150; *Russ. Chem. Bull.*, 42 (1993) 1418–1422.

[20] W. Saenger, in C.R. Cantor (Ed.), *Principles of Nucleic Acid Structure*, Springer, Heidelberg, 1984, pp. 61–65.

[21] S. Cros, C. Herve du Penhoat, S. Pérez, A. Imberty, *Carbohydr. Res.*, 248 (1993) 81–93.
[22] (a) A.D. French, V. Tran, *Biopolymers*, 29 (1990) 1599–1611. (b) S. Immel, *Dissertation*, Technische Hochschule Darmstadt, 1995.
[23] A.D. French, M.K. Dowd, *J. Comput. Chem.*, 15 (1994) 561–570.
[24] (a) H.J. Lindner, M. Kroeker, *PIMM91 — Closed Shell PI–SCF–LCAO–MO–Molecular Mechanics Program*, Darmstadt University of Technology, 1997. (b) A.E. Smith, H.J. Lindner, *J. Comput.-Aided Mol. Des.*, 5 (1991) 235–262.
[25] (a) D. Cremer, J.A. Pople, *J. Am. Chem. Soc.*, 97 (1975) 1354–1358. (b) G.A. Jeffrey, R. Taylor, *Carbohydr. Res.*, 81 (1980) 182–183.
[26] F.H. Allen, O. Kennard, *Chem. Des. Automat. News*, 8 (1993) 1,31–37; *Cambridge Crystallographic Data* File (April 1999), Version 5.17. Refcodes: FACRAC [27], VAJGIW [28], and MACGAL [29].
[27] D. Beer, J.H. Bieri, I. Macher, R. Prewo, A. Vasella, *Helv. Chim. Acta*, 69 (1986) 1172–1190.
[28] P. Köll, J. Kopf, D. Wess, H. Brandenburg, *Liebigs Ann. Chem.*, (1988) 685–693.
[29] P. Beale, N.C. Stephenson, J.D. Stevens, *J. Chem. Soc., Chem. Commun.*, (1971) 25.
[30] (a) H.M. Zuurmond, P.A.M. van der Klein, G.H. Veeneman, J.H. van Boom, *Recl. Trav. Chim. Pays-Bas*, 109 (1990) 437–441. (b) G.H. Veeneman, S. Notermans, P. Hoogerhout, J.H. van Boom, *Recl. Trav. Chim. Pays-Bas*, 108 (1989) 344–350. (c) J. Thiem, H.-P. Wessel, *Liebigs Ann. Chem.*, (1983) 2173–2184. (d) J.E. Nam Shin, A.S. Perlin, *Carbohydr. Res.*, 76 (1979) 165–176. (e) O. Varela, C. Marino, R.M. De Lederkremer, *Carbohydr. Res.*, 155 (1986) 247–251. (f) T. Ziegler, E. Eckhardt, G. Herold, *Liebigs Ann. Chem.*, (1992) 441–451.
[31] H. Gohlke, *Diploma Thesis*, Darmstadt University of Technology, 1997, 69 pp.
[32] (a) N. Metropolis, A.W. Rosenbluth, M.N. Rosenbluth, A. Teller, E. Teller, *J. Chem. Phys.*, 21 (1953) 1087–1092. (b) W.F. van Gunsteren, H.J.C. Berendsen, *Angew. Chem.*, 102 (1990) 1020–1055; *Angew. Chem., Int. Ed. Engl.*, 29 (1990) 992–1023.
[33] H. Goto, E. Osawa, *J. Am. Chem. Soc.*, 111 (1989) 8950–8951.
[34] F.W. Lichtenthaler, S. Immel, *Liebigs Ann. Chem.*, (1996) 27–37; *Starch/Stärke*, 48 (1996) 145–154.
[35] S. Immel, *MolArch$^+$ — MOLecular ARCHitecture Modeling Program*, Darmstadt University of Technology, 1999.
[36] (a) I. Tvaroska, T. Bleha, *Adv. Carbohydr. Chem. Biochem.*, 47 (1989) 45–123. (b) G.E. Schmitt, *Diploma Thesis*, Darmstadt University of Technology, 1995.
[37] M.L. Connolly, *J. Appl. Cryst.*, 16 (1983) 548–558.
[38] J. Brickmann, MOLCAD — MOLecular Computer Aided Design, Darmstadt University of Technology, 1997. The major part of the MOLCAD program is included in the SYBYL package of TRIPOS associates, St. Louis, MI, USA. (b) J. Brickmann, *J. Chim. Phys.*, 89 (1992) 1709–1721. (c) W. Heiden, G. Moeckel, J. Brickmann, *J. Comput.-Aided Mol. Des.*, 7 (1993) 503–514.
[39] M. Teschner, C. Henn, H. Vollhardt, S. Reiling, J. Brickmann, *J. Mol. Graphics*, 12 (1994) 98–105.